Visualizing Individual Rhodopsin (a G Protein-Coupled Receptor) Molecules in Native Disk and Reconstituted Membranes via Atomic Force Microscopy

Eugene J. Choi*, Albert J. Jin*, Shui-Lin Niu**, Paul D. Smith*, and Burton J. Litman**

*IRDR, Division of Bioengineering and Physical Science, ORS, OD, National Institutes of Health, Bethesda, MD, 20892. choieug@ors.od.nih.gov
**Lab Membrane Biochemistry and Biophysics, National Institute of Alcohol Abuse and Alcoholism, National Institutes of Health, Rockville, MD, 20852. litman@helix.nih.gov

ABSTRACT

Individual rhodopsin molecules have been resolved with atomic force microscopy as both monomers and various oligomeric organizations that are sensitively dependent upon the physical state of membranes and environmental conditions. In intact native disk membranes, rhodopsin molecules are observed as randomly dispersed monomers and small oligomers. In reconstituted rhodopsin-DPPC (dipalmitoylphosphatidylcholine, di16:0-PC) membranes, phase separation of lipid and rhodopsin results in paracrystalline arrays of rhodopsin molecules. Since the coupling of rhodopsin and G proteins is an essential step in visual transduction, the results from this study could provide further insight into the structural relationship of rhodopsin to its function in vision and may have applications in nanotechnology.

Keywords: atomic force microscopy, rhodopsin, G-protein-coupled receptor, cell membrane.

1 INTRODUCTION

The rod outer segment (ROS) contains a stack of densely-packed, closed, flattened membrane disks [1]. These ROS disk membranes contain lipids and proteins, with docosahexaenoic acid (DHA) being the dominant phospholipid acyl chains and rhodopsin representing 95% of the protein content and acting as an important component for visual function [1]. Rhodopsin is a prototypical member of the heptahelical G-protein coupled receptor family, which is the largest family of cell surface receptors. The visual signal transduction pathway is initiated when a photon of light is absorbed by rhodopsin, resulting in the formation of metarhodopsin II, the G protein activating form of rhodopsin, from the inactive metarhodopsin I [1]. This transition promotes the binding and activation of the G protein transducin, which activates a phosphodiesterase, initiating the hydrolysis of cGMP and leading to Na^{+}/Ca^{+2} channel closures, resulting in a hyperpolarization of the plasma membrane transmitted to the synapse of the rod cell [1].

The structure and function of bovine rhodopsin are well characterized and studied [1-3]. However, the molecular organization of rhodopsin in disk membranes, which can have a critical impact on protein-protein interactions, was not directly observed until recently. Rhodopsin molecules from wild-type mouse ROS disk membranes were resolved as dimers organized in paracrystalline arrays on the cytoplasmic side of opened, single-layered disk membranes using atomic force microscopy [4].

Atomic force microscopy (AFM) is an innovative form of scanning probe microscopy with increasingly broad biological applications [e.g. 4, 5]. A sharp tip attached to the end of a cantilever is scanned across a surface permitting both atomic interactions between the probe and sample to be measured and sub-nanometer structures in biological samples *in situ* to be resolved. With specific advancements in AFM instrumentation, we have resolved bovine rhodopsin molecules on the top surface of intact ROS disks and have observed spontaneous phase separation of rhodopsin and lipid in reconstituted rhodopsin-DPPC membranes. In this manner, the organization of rhodopsin is captured in its most natural state, and its interplay with lipid environment is accessed.

2 EXPERIMENTAL

The ROS membranes were isolated from bovine retinas using the modified Shake-ate method [6]. Intact ROS disk membranes were isolated from ROS membranes using the Ficoll-floatation method [7]. Rhodopsin was purified on a conA affinity column [8]. Reconstituted rhodopsin-DPPC membranes were prepared using the dilution reconstitution method [9].

For AFM measurements, the ROS disk membranes and the reconstituted rhodopsin-DPPC membranes in large unilamellar vesicle (LUV) suspensions (c.a. 100 nm diameter via extrusion procedure) were adsorbed on mica in 5 mM Tris, 50 μM DTPA, 2mM DTT buffer and then washed with 20 mM Tris, 150 mM NaCl, 25 mM $MgCl_2$, 50 μM DTPA, 2

mM DTT. All imaging was performed under similar high ionic strength buffers and at room temperature, in both dark and light conditions, with the future capability of environmental control with argon gas. Both contact mode and tapping mode (TM) were utilized in this study with a PicoForce Multimode AFM under a Nanoscope IV controller and either a PicoForce or a type E scanner head (Veeco/Digital Instruments, CA) [5].

3 RESULTS & DISCUSSION

3.1 Rhodopsin in ROS Native Disk

This study shows, for the first time, individually resolved rhodopsin molecules on an intact, double-layered native membrane disk. AFM images (Figures 1A and 1B) reveal circular intact native disks with thicknesses between 13-18 nm and diameters of about 1 μm (Figure 1C). These thickness values are consistent with a height of two bilayer membranes stacked on top of each other, indicating that the disks are intact. Densely-packed rhodopsin molecules in close contact with each other can be seen on the surface of the disk membrane, and higher resolution low-pass filtered scans reveal that rhodopsin molecules are distributed in a random manner in the native disk as monomers and small oligomers (not shown). This random rhodopsin organization, as also evidenced by calculated power spectra (not shown), is contrary to the paracrystalline organization observed in single-layered disks from mice [4], but is consistent with historical biophysical and biochemical observations of random and diffusive rhodopsin dispersion in the fluid-like lipid environment of disk membranes provided by the high level of DHA phospholipids [10]. This discrepancy could be attributed to the effect of the mica substrate, which clearly caused lipid phase separation in the single-layered disks [4,10]. In our study, the images are obtained from the upper bilayer of the double-layered intact bovine disk, which is not in direct contact with the mica surface.

A typical AFM force spectroscopy curve (Figure 1D) shows that rhodopsin molecules in native disks can be stretched up to 120 nm, which is consistent with the full length of the extended rhodopsin peptide chain. The initial force needed to unfold and stretch the rhodopsin is about 500 pN. The cantilever then retracts and a smaller force of about 250 pN is sufficient to unfold the rest of the rhodopsin, comparable to other proteins [11].

The conditions necessary for optimal adsorption of the native disk to mica substrate required the use of high ionic strength buffer and the presence of monovalent and divalent ions. It is important to have native intact disk membranes adsorbed strongly enough to the mica support, but not so strong as to disrupt and burst the disks. This type of adsorption allows molecular rhodopsin to be visualized in the upper membrane by AFM. Our high ionic strength buffer conditions with divalent ions are similar to conditions used by Fotiadis *et al.* [4] when they observed paracrystalline arrays of rhodopsin dimers in single-layered disks.

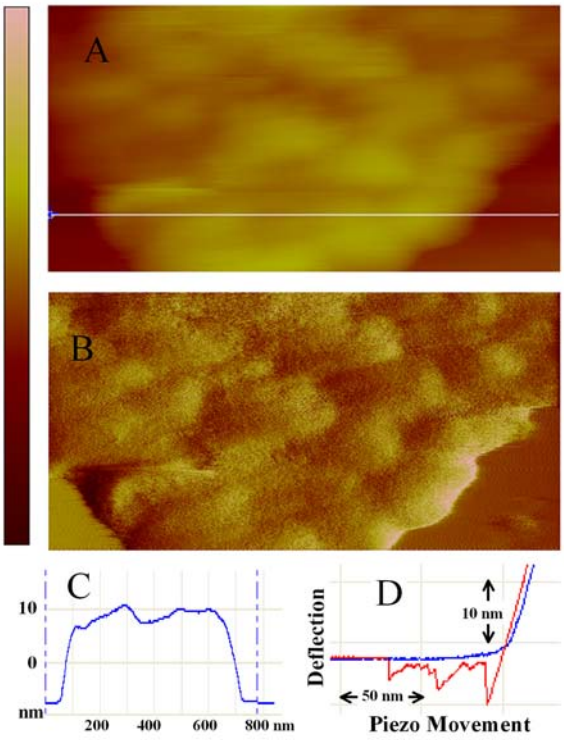

Figure 1: Examples of AFM measurements of native disk membranes with rhodopsin molecules in dark state at room temperature. **(A)** A contact-mode topographic image of a bovine ROS native disk membrane adsorbed on mica-supported surface (450 nm × 900 nm). **(B)** The deflection image corresponding to (A), showing both the densely-packed rhodopsin molecules and the smooth mica surface (on the left and right bottom corners of the figure). The brightness scales (top left) for height contrast in A and B is 60 nm and 1 nm, respectively. **(C)** A section profile corresponding to the white line in Figure 1A, confirming the presence of intact double bilayers in our disk preparations. **(D)** An example of an AFM force spectroscopy curve consistent with the unfolding of rhodopsin trans-membrane helices (blue curve for approaching; red curve for retraction and stretching). The nominal cantilever spring constant is 50 pN/nm.

3.2 Reconstituted Rhodopsin-DPPC

To address the issue of ROS disk adsorption and the interplay of rhodopsin organization with lipid phase separation on mica, this study now focuses on a reconstituted system with controlled rhodopsin to lipid ratios. Individual rhodopsin molecules were resolved by TM AFM in reconstituted rhodopsin-DPPC membranes with rhodopsin to DPPC ratios of 1:100 and 1:200. Under low ionic strength buffer conditions, the reconstituted membranes only weakly

adsorb to the mica surface. However, as with the native disk membrane, the reconstituted rhodopsin-DPPC lipid membranes adsorbed more strongly to mica in the presence of high ionic strength buffer with both monovalent and divalent ions. At molar ratios of 1:100 and 1:200 [rhodopsin:DPPC] on mica (Figures 2 and 3), phase separation between rhodopsin-rich areas and rhodopsin-poor regions of the DPPC could be observed, with individual rhodopsin molecules being resolved. The rhodopsin-rich membrane is about 1-3 nm thicker than the surrounding membrane of thickness of 4-5 nm (Fig. 2A-C). Both rhodopsin monomers and oligomeric organizations occur in these rhodopsin-rich domains (Figure 3).

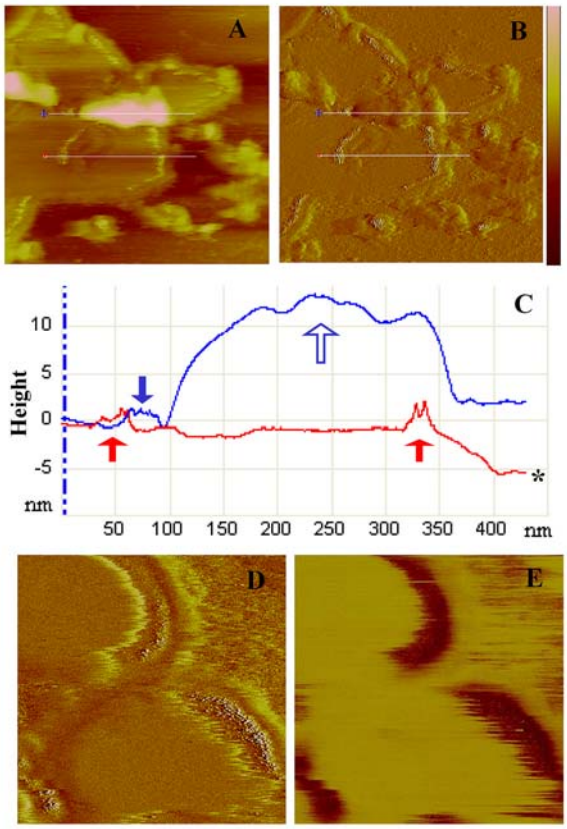

Figure 2: Phase separation in reconstituted rhodopsin-DPPC [1:100] membranes on mica substrates under light state at room temperature. **(A)** TM topographic image of a large rhodopsin-DPPC membrane region that contains elongated domains of rhodopsin monomers in DPPC bilayer as well as larger aggregates (0.75µm ×0.75µm scan). **(B)** TM amplitude map corresponding to (A). **(C)** Section profiles (lines in (A and B) with blue and red +) with filled arrows pointing to monomeric rhodopsin, and an open arrow pointing to larger multilayer membranes or rhodopsin aggregates. The mica substrate is indicated by *. **(D)** TM amplitude map of two un-fused liposome patches with phase separations (0.25µm ×0.25µm). **(E)** The corresponding phase image map showing huge AFM TM cantilever oscillation phase delay over rhodopsin-rich membrane, but not over rhodopsin-poor membrane (upper left and center) or bare mica substrate (upper right). The brightness scale (top right) for (A), (B), (D), (E) is 20 nm, 300mV, 250mV, and 60 degrees.

The oscillation phase lag of the cantilever resonance relative to the signal sent to the cantilever's piezoelectric driver is an important measure of the viscoelastic and adhesion properties of the membrane. Figure 2E shows the first observations of membrane phase separation, into rhodopsin-rich areas and rhodopsin-poor areas, as measured with phase imaging using TM AFM. This technique provides clear resolution of membrane domains with substantial differences in material properties, and features that can be obscured by rough topography in height images. While structural details generally are revealed more clearly in error maps such as Figures 2B and 2D, TM AFM phase imaging is a powerful tool for displaying variations in sample properties both at very high resolution and in real time. At room temperature, the DPPC-rich phase is in the gel state, resulting in higher rhodopsin stability and lower rhodopsin mobility. This is in contrast to the native disk condition in which DHA phospholipids are highly unsaturated and more fluid, resulting in lower rhodopsin stability [3]. Tokumasu *et al.* have demonstrated that the phase behavior in supported reconstituted DPPC, dilauroylphosphatidylcholine, and cholesterol mixture membranes is modified compared with unsupported mixture membranes due to effects from the mica substrate. These mica effects depend on such factors as type and ratio of lipid mixtures, concentrations of monovalent and divalent ions, and buffer pH over the mica surface [5]. Our results show that rhodopsin-DPPC membrane phase separation occurs in single bilayers adsorbed to mica (Fig. 2).

In Figure 3A, regions of individual rhodopsin monomers can be clearly observed in the rhodopsin-rich phase at molar ratio [1:200]. Within this phase, individual rhodopsin molecules could be resolved with monomer peak spacing of about 3.5 nm (Figure 3B). Rhodopsin molecules packed together can be observed more clearly in Figures 3C and D, suggesting a structured organization. At a molar ratio of [1:200] of rhodopsin-DPPC membrane, two populations of rhodopsin molecules with different protrusion heights and shapes can be discerned in their respective arrays (Figures 3C). At the higher ratio of [1:100], two similar populations of individual rhodopsin molecules are evident although the structured arrays are less extensive (Figure 3D). This could reflect the non-vectorial incorporation of rhodopsin molecules in the LUV bilayers during reconstitution resulting in surface exposure of both the C- and N-terminal ends of the protein. The different extent of array formation may reflect a better membrane stress energy release in the lower rhodopsin composition. Indeed, topographic image maps corresponding to Figures 3D (not shown) reveal two protrusion classes of equal numbers of molecules with respective protrusion heights of about 0.9 nm and 1.9 nm over the surrounding membrane. The paracrystalline array structure observed here is similar to that observed in the single-layered disk studied

by Fotiadis *et al.* [4], indicating that the crystalline structure may be a result of the above-mentioned phase separation [10].

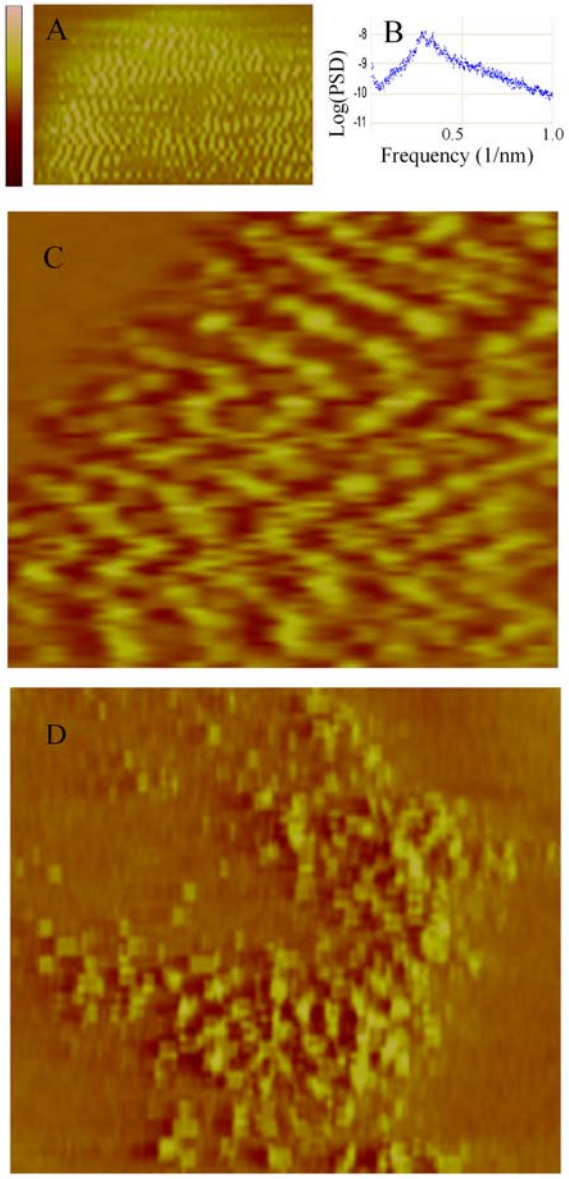

Figure 3: Molecular organization of rhodopsin molecules in reconstituted rhodopsin-DPPC membranes under light state at room temperature. **(A)** TM topographic image of reconstituted rhodopsin-DPPC [1:200] membranes (75 nm × 75 nm). **(B)** Horizontal 2D power spectrum of (A), showing rhodopsin spacing peaks at about 3.5 nm. **(C)** High-resolution low-pass filtered TM amplitude image of rhodopsin molecules in rhodopsin-DPPC [1:200] membrane (50 nm horizontally). Two different molecular shapes can be identified, and they each tend to form distinct arrays. **(D)** High resolution low-pass filtered TM amplitude images of rhodopsin molecules in rhodopsin-DPPC [1:100] membranes (50 nm horizontally). Molecular arrays are less extensive, but two classes of the molecular protrusion height and shape can still be identified. The brightness scale (top left) for height contrast in A, C and D is 20 nm, 500 mV and 400 mV, respectively.

4 SUMMARY

For the first time, individual rhodopsin molecules were resolved in both the intact native disk membrane and the reconstituted rhodopsin-DPPC membranes using AFM. Unlike the random distribution in the intact native disk membrane with rhodopsin molecules in close yet transient associations, rhodopsin molecules in the reconstituted system are organized in a paracrystalline pattern and as monomers and oligomers that may depend on membrane phase separation, caused by direct interaction with the mica substrate. Our images obtained in native disk membranes arise from sampling the upper membrane surface of the disk, which is not in direct contact with the mica surface.

The results of this study should give further insight on the relationship between vision disk membrane structure and function. By manipulating the phase behavior between rhodopsin and membranes, one could control the lateral organization of rhodopsin for use in a smart device, molecular motor, or other bio- and nanotechnology applications.

5 ACKNOWLEDGEMENTS

We thank Sylvain Ho, Ed Wellner and Dr. Emilios Dimitriadis for contributions toward improving the AFM facility at DBEPS/ORS/OD/NIH.

6 REFERENCES

[1] Albert, A. D., Yeagle, P. L. (2002) *Biochim. Biophys. Acta* 1565, 183.
[2] Sakmar *et al.* (2002) *Annu. Rev. Biophys. Biomol. Struct.* 31, 443.
[3] Polozova, A., Litman, B. J. (2000) *Biophys. J.* 79, 2632.
[4] Fotiadis *et al.* (2003) *Nature* 421, 127.
[5] Tokumasu *et al.* (2003) *Biophys. J.* 84, 1.
[6] Miller *et al.* (1986) *Biochemistry* 25, 4983.
[7] Smith, H.G., Litman, B.J. (1982) *Methods Enzymol* 81, 57.
[8] Litman, B.J. (1982) *Methods Enzymol* 81, 150.
[9] Jackson, M.L., Litman, B.J. (1985) *Biochi.Biophys. Acta* 812, 369.
[10] Chabre *et al.* (2003) *Nature* 426, 30.
[11] Wang *et al.* (2001). *Prog. Biophys. Molec. Biol*. 77**,** 1.